Journal of Applied Fluid Mechanics, Vol. 8, No. 2, pp. 273-280, 2015.
Available online at www.jafmonline.net, ISSN 1735-3572, EISSN 1735-3645.
DOI: 10.18869/acadpub.jafm.67.221.22846

Flow of Power-Law Nanofluid over a Stretching Surface with Newtonian Heating

T. Hayat[1,2], M. Hussain[3], A. Alsaedi[2], S. A. Shehzad[5†] and G. Q. Chen[2,4]

[1]*Department of Mathematics, Quaid-I-Azam University 45320, Islamabad 44000, Pakistan*
[2]*Department of Mathematics, Faculty of Science, King Abdulaziz University, P. O. Box 80203, Jeddah 21589, Saudi Arabia*
[3]*University of Engineering and Technology (RCET Campus), Lahore 54890, Pakistan*
[4]*College of Engineering, Peking University, Beijing, China*
[5]*Department of Mathematics, Comsats Institute of Information Technology, Sahiwal, 57000, Pakistan*

†*Corresponding Author Email:* ali_qau70@yahoo.com

(Received March 20, 2014; accepted April 30, 2014)

ABSTRACT

The present investigation addresses the effect of Newtonian heating in the laminar flow of power law nanofluid. The flow is induced by a stretching surface. The nonlinear analysis comprising flow and energy equations is computed. The problems are solved for the series solutions of velocity and temperature. Skin friction coefficient and Nusselt number are computed. A parametric study is performed for the influential parameters on the velocity and temperature. Physical interpretation of the derived solutions is presented.

Keywords: Power-law nanofluid; Pade approximation; Newtonian heating.

NOMENCLATURE

u, v	velocity components	ρ_{nf}	effective density
μ_{nf}	effective dynamic viscosity	T	temperature
h_s	heat transfer coefficient	k	power law index
g	gravitational acceleration	β_{nf}	thermal expansion coefficient
α_{nf}	effective thermal diffusivity	k_{nf}	effective thermal conductivity
ϕ	nanoparticle volume fraction	ψ	stream function
η	dimensionless variable	Re_x	local Reynolds number
f	dimensionless velocity	θ	dimensionless temperature
$N\,Pr$	modified Prandtl number	λ	buoyancy parameter
γ	Newtonian heating parameter	Gr_x	local Grashoff number
T_w	temperature at wall	T_∞	ambient fluid temperature

1. INTRODUCTION

The dynamics of nanofluids is thrust area of current research. Such fluids have greatly received the attention of recent investigators due to their enhanced thermal conductivity property. In fact the fluid heating and cooling have importance in the manufacturing, power and transportation industries. There is a great need regarding the efficient mechanisms for cooling any sort of high energy device. The usual heat transfer base fluids in view of their low heat transfer characteristics do not possess effective heat transfer capabilities. The metals considered have three times higher thermal conductivities than such fluids. Thus combination of two substances is desired to produce heat transfer medium that behaves as a fluid but has thermal of a metal. A fluid consisting of nano-sized particles is known as nanofluid. Such fluids are engineered colloidal suspensions of nanoparticles in a base fluid. The commonly used based fluids are water, oil, lubricants, ethylene glycol, toluene, biofluids and polymer solutions whereas the nanoparticles are made of metals (gold, aluminium, copper, iron, titanium, methanol), oxides (Al_2O_3), carbides (SiC), nitrides (AIN, SiN) or non-metals (Graphite, Carbon nanotubes). The selection of base fluid particle combination depends upon the application for which the

nanofluid is intended. Nanoparticles range in diameter between 1 and 100 nm. In particular the nanofluids are useful in several processes including fuel cells, microelectronics, hybrid-powered engines, pharmaceutical processes etc. Involvement of nanoparticles is of highly scientific interest because they provide a bridge between bulk materials and nanoparticles structures. Choi (1995) in the experimental study of nanofluids analyzed that the nanoparticles are best candidate to enhance the thermal conductivity and heat transfer rate. Afterwards different theoretical investigations have been carried out for nanofluids under several flow configurations. For example Makinde and Aziz (2011) studied the boundary layer flow of nanofluid over a flat plate with convective condition. Mustafa et al. (2011) analyzed the stagnation point flow of nanofluid over a stretching surface. Turkyilmazoglu (2012a) developed exact analytical solutions for the flow of nanofluid with heat and mass transfer in the presence of slip condition. Sheikholeslami et al. (2013a) studied the magnetohydrodynamic flow of nanofluid in channel. Entropy generation analysis in MHD steady flow of nanofluid over a rotating disk has been presented by Rashidi et al. (2013). Thermal radiation effect in the viscous-nanofluid flow over nonlinear stretching sheet was discussed by Hady et al. (2012).

Mixed convection flow of nanofluid with heat transfer occurs in many physical and engineering applications like chemical catalytic reactors, fiber and granular insulation, geothermal systems, nuclear waste repositories and many others. Oztop et al. (2011) performed a computational analysis for natural convection nanofluid flow in the presence of non-isothermal temperature distribution. Chamkha and Abu-Nada (2012) studied the mixed convection flow of AL_2O_3 nanofluid filled in a single and double lid-driven cavities. Turkyilmazoglu and Pop (2013) discussed the natural convection flow of nanofluid with heat and mass transfer over a vertical plate in the presence of thermal radiation. Effect of double-stratification in natural convection flow of nanofluid with heat transfer was numerically studied by Ibrahim and Makinde (2013). Hady et al. (2011) analyzed the effect of heat source/sink in natural convection boundary layer flow of nanofluid over a vertical cone. Hamad (2011) developed the analytical solutions for natural convection flow of nanofluid in the presence of applied magnetic field. Natural convection flow of nanofluid in a cavity with sinusoidal wall was examined by Sheikholeslami et al. (2013b).

Recently Newtonian heating gains much more attention of the investigators due to its engineering and industrial applications. Examples of such applications are heat exchanger, solar radiation, petroleum industry, conduction within the fin etc. Salleh et al. (2010) investigated the boundary layer flow of viscous fluid over a surface in the presence of Newtonian heating. Hayat et al. (2012a) extended the analysis of Salleh et al. (2010) for second grade fluid. MHD unsteady flow of viscous fluid with Newtonian heating and Navier-slip was numerically discussed by Makinde (2012). Ramzan et al. (2013) carried out an analysis to study the Newtonian heating effects in three-dimensional boundary layer flow of couple stress fluid over a stretching surface. Shehzad et al. (2014) studied the three-dimensional flow of Jeffrey fluid in the presence of Newtonian heating.

The purpose of present investigation is to analyze the boundary layer flow of power law nanofluid over a vertical stretching sheet. Heat transfer analysis is taken in the presence of Newtonian heating. To the best of author knowledge such investigation is not available in the literature yet. Series solutions are computed for the velocity and temperature via homotopy analysis method (HAM) (Liao (2003), Rashidi and Domairry (2009), Rashidi et al. (2011), Keimanesh et al. (2011), Turkyilmazoglu (2012b), Hayat et al. (2012b), Rashidi et al. (2012a,b), Abbasbandy et al. (2013) and Hayat et al. (2013a,b)). Results for physical parameters namely nanoparticle volume fraction, buoyancy parameter, modified Prandtl number and Newtonian heating parameter are plotted and analyzed. Graphical results for skin-friction coefficient and Nusselt number are also examined.

1. PROBLEM STATEMENT

Let us consider the two-dimensional laminar boundary layer flow of non-Newtonian fluid with nanoparticles. Constitutive relations of power law fluid are under examination. The $x-$axis is taken along the surface while the $y-$axis is normal to it. Two equal and opposite forces act along the surface so that the wall is stretched linearly by keeping the origin fixed. The velocity and temperature associated to the surface are u_w and T_w respectively. The ambient fluid temperature is denoted by T_∞. Further the regular fluid and the nanoparticles are taken in thermal equilibrium. The surface also exhibits the Newtonian heating effects. The relevant boundary value problems can be put into the forms:

$$\frac{\partial u}{\partial x}+\frac{\partial v}{\partial y}=0, \tag{1}$$

$$u\frac{\partial u}{\partial x}+v\frac{\partial u}{\partial y}=\frac{1}{\rho_{nf}}\begin{pmatrix}-\mu_{nf}\frac{\partial}{\partial y}\left(-\frac{\partial u}{\partial y}\right)^k\\ \pm g(\rho\beta)_{nf}(T-T_\infty)\end{pmatrix}, \tag{2}$$

$$u\frac{\partial T}{\partial x}+v\frac{\partial T}{\partial y}=\alpha_{nf}\frac{\partial^2 T}{\partial y^2}, \tag{3}$$

$$u=bx,\ v=0,$$

$$\frac{\partial T}{\partial y}=-hsT,\ at\ y=0, \tag{4}$$

$$u\to 0,\ T\to T_\infty\quad as\ y\to\infty,$$

where u and v are the velocity components in the x and y-directions, μ_{nf} denotes the effective dynamic velocity, T the temperature of fluid, h_s the specific heat transfer parameter, k the power law index, g the gravitational acceleration, ρ_{nf} effective density, β_{nf} the thermal expansion coefficient, α_{nf} the effective

thermal diffusivity and k_{nf} is the effective thermal conductivity of nanofluid. We have

$$\begin{aligned}
&\rho_{nf} = (1-\varphi)\rho_f + \varphi\rho_s,\ \mu_{nf} = \frac{\mu_f}{(1-\varphi)^{2.5}},\\
&(\rho\beta)_{nf} = (1-\varphi)(\rho\beta)_f + \varphi(\rho\beta)_s,\\
&(\rho C_p)_{nf} = (1-\varphi)(\rho C_p)_f + \varphi(\rho C_p)s,\\
&\alpha_{nf} = \frac{k_{nf}}{(\rho C_p)_{nf}},\\
&k_{nf} = k_f\left(\frac{k_s + 2k_f - 2\varphi(k_f - k_s)}{k_s + 2k_f - 2\varphi(k_f - k_s)}\right).
\end{aligned} \tag{5}$$

in which φ is the solid volume fraction of the nanoparticles. Writing

$$\begin{aligned}
&\Psi = xu_w(\mathrm{Re}_x)^{-1/(k+1)} f(\eta),\\
&\eta = \frac{y}{x}(\mathrm{Re}_x)^{-1/(k+1)},\ \theta(\eta) = \frac{T - T_\infty}{T_\infty},
\end{aligned} \tag{6}$$

where $\Psi(x,y)$ is the stream function, Re is the local Reynolds number and $u = \frac{\partial\Psi}{\partial y}, v = -\frac{\partial\Psi}{\partial x}$ we have from Eqs. (2)-(4) as follows

$$\begin{aligned}
&\frac{k}{(1-\varphi)^{2.5}}[-f'']^{k-1} f''' + (1 - \varphi + \varphi(\rho_s/\rho_f))\\
&\left(\frac{2k}{k+1} ff'' - f'^2\right)\\
&+\lambda(1 - \varphi + \varphi((\rho\beta)_s/(\rho\beta)_f))\theta = 0,
\end{aligned} \tag{7}$$

$$\begin{aligned}
&\frac{1}{N\,\mathrm{Pr}}\left(\frac{k_{nf}}{k_f}\right)\varphi'' + (1 - \varphi + \varphi((\rho C_p)_s/(\rho C_p)_f))\\
&\left(\frac{2k}{1+k}\right) f\theta' - f'\theta = 0,
\end{aligned} \tag{8}$$

$$\begin{aligned}
&f(0) = 0,\ f'(0) = 1,\ \theta'(0) = -\gamma(1 + \theta(0)),\\
&f'(\eta) = 0,\ \theta(\eta) = 0\ \ as\ \ \eta \to \infty,
\end{aligned} \tag{9}$$

where Eq. (1) is satisfied identically, prime signifies differentiation with respect to η and

$$\begin{aligned}
&N\,\mathrm{Pr} = \frac{bx^2}{\alpha f}(\mathrm{Re}_x)^{-2/(k+1)},\ \lambda = \pm Gr_x/\mathrm{Re}_x,\\
&Gr_x = g\beta(Tw - T_\infty)xb^{-n}/\nu_f, \gamma = h_s(\nu/a)^{1/2}.
\end{aligned} \tag{10}$$

In above Eq. $N\,\mathrm{Pr}$ is the modified Prandtl number for power law fluid, λ is the buoyancy parameter. Here $\lambda > 0$ corresponds to buoyancy assisting flow and $\lambda < 0$ the buoyancy opposing flow, Gr_x the local Grashoff number and γ the Newtonian heating parameter.

The skin friction coefficient C_f and the local Nusselt number Nu_x are presented into the forms

$$\begin{aligned}
&C_f = \frac{2\mu_{nf}}{\rho_f u_w^2}\left(\left.\frac{\partial u}{\partial y}\right|_{y=0}\right)^k,\\
&Nu_x = \frac{xk_{nf}}{k_f(Tw - T_\infty)}\left(\frac{\partial T}{\partial y}\right)_{y=0}.
\end{aligned} \tag{11}$$

Equations (10) and (11) in nondimensionalized form can be written as

$$(\mathrm{Re}_x)^{-1/(k+1)} C_f = \frac{2}{(1-\varphi)^{2.5}}[-f''(0)]^k, \tag{12}$$

$$(\mathrm{Re}_x)^{-1/(k+1)} Nu_x = \gamma\left(1 + \frac{1}{\theta(0)}\right)\frac{k_{nf}}{k_f}. \tag{13}$$

2. DEVELOPMENT OF SERIES SOLUTIONS

The adopted initial guesses (f_0, θ_0) and auxiliary linear operators (L_f, L_θ) here are

$$f_0(\eta) = 1 - e^{-\eta},\ \theta_0(\eta) = \frac{\gamma * e^{-\eta}}{1-\gamma}, \tag{14}$$

$$L_f = \frac{d^3 f}{d\eta^3} + \frac{d^2 f}{d\eta^2},\ L_\theta = \frac{d^2\theta}{d\theta^2} - \theta \tag{15}$$

with the properties

$$L_f\left[C_1 + C_2\eta + C_3 e^{-\eta}\right] = 0,\ L_\theta\left[C_4 e^{\eta} + C_5 e^{-\eta}\right] = 0, \tag{16}$$

in which C_i $(i = 1-5)$ are the arbitrary constants. Defining $p \in [0,1]$ as an embedding parameter and $(\hbar_f, \hbar_\theta)$ the nonzero auxiliary parameters we have the following zeroth order problem in the forms:

$$\begin{aligned}
&(1-p)L_f[\hat{f}(\eta;p) - f_0(\eta)]\\
&= p\hbar_f \mathbf{N}_f\left[\hat{f}(\eta;p)\right],
\end{aligned} \tag{17}$$

$$\begin{aligned}
&(1-p)L_\theta[\hat{\theta}(\eta;p) - \theta_0(\eta)]\\
&= p\hbar_\theta \mathbf{N}_\theta\left[\hat{f}(\eta;p), \hat{\theta}(\eta;p)\right],
\end{aligned} \tag{18}$$

$$\begin{aligned}
&\hat{f}(\eta,p)\big|_{\eta=0} = 0,\ \left.\frac{\partial\hat{f}(\eta,p)}{\partial\eta}\right|_{\eta=\infty} = 1,\\
&\hat{\theta}'(\eta,p)\big|_{\eta=0} = -\gamma(1 + \theta(0)),\\
&\left.\frac{\partial\hat{f}(\eta,p)}{\partial\eta}\right|_{\eta=\infty} = 0,\ \hat{\theta}(\eta,p)\big|_{\eta=\infty} = 0.
\end{aligned} \tag{19}$$

For $k = 1$ the nonlinear operators are represented by

$$\begin{aligned}
&\mathbf{N}_f\left[\hat{f}(\eta;p), \hat{g}(\eta;p)\right] =\\
&\frac{1}{(1-\phi)^{2.5}}\frac{\partial^3\hat{f}(\eta;p)}{\partial\eta^3}\\
&+[1 - \phi + \phi(\rho_s/\rho_f)]\hat{f}(\eta;p)\frac{\partial\hat{f}(\eta;p)}{\partial\eta}\\
&-\left(\frac{\partial\hat{f}(\eta;p)}{\partial\eta}\right)^2 + \lambda[1 - \phi + \phi((\rho\beta)_s/(\rho\beta)_f)]\theta,\\
&\mathbf{N}_\theta\left[\hat{f}(\eta;p), \hat{\theta}(\eta;p)\right] =
\end{aligned} \tag{20}$$

$$\frac{1}{N\,\mathrm{Pr}}\left(\frac{k_{nf}}{k_f}\right)\frac{\partial^2\hat{\theta}(\eta;p)}{\partial\eta^2}$$
$$+[1-\varphi+\varphi((\rho C_p)_s/(\rho C_p)_f)] \tag{21}$$
$$\hat{f}(\eta;p)\frac{\partial\hat{\theta}(\eta;p)}{\partial\eta}-\hat{\theta}(\eta;p)\frac{\partial\hat{f}(\eta;p)}{\partial\eta}.$$

For $p=0$ and $p=1$ one can write

$$\hat{f}(\eta;0)=f_0(\eta),\quad \hat{f}(\eta;1)=f(\eta), \tag{22}$$
$$\hat{\theta}(\eta;0)=\theta_0(\eta),\quad \hat{\theta}(\eta;1)=\theta(\eta), \tag{23}$$

and expressions of $\hat{f}$ and $\hat{\theta}$ are

$$\hat{f}(\eta;p)=f_0(\eta)+\sum_{m=1}^{\infty}f_m(\eta)p^m, \tag{24}$$
$$\hat{\theta}(\eta;p)=\theta_0(\eta)+\sum_{m=1}^{\infty}\theta_m(\eta)p^m, \tag{25}$$
$$f_m(\eta)=\frac{1}{m!}\frac{\partial^m f(\eta;p)}{\partial\eta^m}\bigg|_{p=0},$$
$$\theta_m(\eta)=\frac{1}{m!}\frac{\partial^m\theta(\eta;p)}{\partial\eta^m}\bigg|_{p=0}. \tag{26}$$

The values of $\hbar_f$ and $\hbar_\theta$ are selected in such a way that the series solutions are convergent at $p=1$ then

$$f(\eta)=f_0(\eta)+\sum_{m=1}^{\infty}f_m(\eta), \tag{27}$$
$$\theta(\eta)=\theta_0(\eta)+\sum_{m=1}^{\infty}\theta_m(\eta). \tag{28}$$

The $mth-$ order deformation problems are given by

$$L_f\left[f_m(\eta)-\chi_m f_{m-1}(\eta)\right]=\hbar_f\mathbf{R}_m^f(\eta), \tag{29}$$
$$L_\theta\left[\theta_m(\eta)-\chi_m\theta_{m-1}(\eta)\right]=\hbar_\theta\mathbf{R}_m^\theta(\eta), \tag{30}$$
$$f_m(0)=0,\ f_m'(0)=0,\ f_m'(\infty)=0,$$
$$\theta_m'(0)=\theta_m(\infty)=0. \tag{31}$$

For $k=1,2$ the nonlinear operators are given below:

$$\mathbf{R}_m^f(\eta)=\frac{1}{(1-\varphi)^{2.5}}f_{m-1}'''+[1-\varphi+\varphi(\rho_s/\rho_f)]$$
$$\sum_{k=0}^{m-1}f_k f_{m-1-k}''-[1-\varphi+\varphi(\rho_s/\rho_f)] \tag{32}$$
$$\sum_{k=0}^{m-1}f_k' f_{m-1-k}'+\lambda\theta_{m-1},$$

$$\mathbf{R}_m^\theta(\eta)=\frac{1}{N\,\mathrm{Pr}}\left(\frac{k_{nf}}{k_f}\right)\theta_{m-1}'' \tag{33}$$
$$+[1-\varphi+\varphi((\rho C_p)_s/(\rho C_p)_f)]$$
$$\sum_{k=0}^{m-1}f_k\theta_{m-1-k}'-\sum_{k=0}^{m-1}\theta_k f_{m-1-k}', \tag{34}$$

$$\chi_m=\begin{cases}0, & m\le 1,\\ 1, & m>1.\end{cases} \tag{35}$$

The general solutions of Eqs. (27) and (28) are

$$f_m(\eta)=f_m^*(\eta)+C_1+C_2\exp(\eta)+C_3\exp(-\eta), \tag{36}$$
$$\theta_m(\eta)=\theta_m^*(\eta)+C_4\exp(\eta)+C_5\exp(-\eta), \tag{37}$$

in which $f_m^*(\eta)$ and $\theta_m^*(\eta)$ are the particular solutions of Eqs. (27) and (28) Note that Eqs. (32) – (34) can be solved by means of any symbolic onal software like Maple Mathematica etc (20) the other in the order $m=1,2,3,...$

3. CONVERGENCE AND ANALYSIS OF THE DERIVED DOLUTIONS

The series solution (27) and (28) consists of the auxiliary parameters $\hbar_f$ and $\hbar_\theta$ which guarantee the convergence of the solutions. In order to find the proper values of $\hbar_f$ and $\hbar_\theta$ we have sketched the $\hbar-$curves of $\hbar_f$ and $\hbar_\theta$ at 20^{th} order of approximations (see Figs. 1 and 2). These Figs. depict that the appropriate values of $\hbar_f$ and $\hbar_\theta$ are $-1.65\le\hbar_f\le-0.5$ and $-1.81\le\hbar_\theta\le-0.4$ respectively. Table 1 is obtained through Pade-approximation at different values of emerging parameters. Table 1 witness that at 20^{th} order of approximation the series solutions are convergent. Table 2 presents the numerical values of local Nusselt number $(\mathrm{Re}_x)^{-1/(k+1)}Nu_x$ of Cu-water nanofluid for different values of *NPr*, λ and γ when *k=1.0* and *k=2.0*. We examined that the values of local Nusselt number are larger for *k=2.0* in comparison to values at *k=1.0*.

Our next concern is to perform a parametric study of the influential parameters on the velocity and temperature. Hence the velocity profile $f'(\eta)$ for different values of volume fraction of nanoparticles φ is displayed in Fig. 3. It is clear that with an increase in the values of φ the velocity and associated boundary layer thickness decrease. Effects of buoyancy parameter λ on the velocity profile $f'(\eta)$ are shown in Fig. 4. Velocity $f'(\eta)$ increases by increasing the values of λ. The value $\lambda=-2$ is for the buoyancy assisting flow and positive values of λ are for the buoyancy opposing flow. We observed that the velocity is lower for buoyancy opposing flow in comparison to the buoyancy assisting flow. The buoyancy force is stronger for the assisting flow and weaker for the opposing flow. Fig. 5 is prepared to see the effects of Newtonian heating parameter γ on the dimensionless temperature $\theta(\eta)$. It is noted that an increase in the values of γ leads to an enhancement in the temperature and thermal boundary layer thickness. Newtonian heating parameter depends upon the heat transfer coefficient. An increase in the values of Newtonian heating parameter gives rise to the heat transfer coefficient. This increase in heat transfer coefficient is responsible for the enhancement in temperature and thermal boundary layer thickness. Fig. 6 is plotted to see the effects of volume fraction of nanoparticles φ on the temperature $\theta(\eta)$. It is observed that $\theta(\eta)$ increases when the values of φ are increased. Variation

of modified Prandtl number $N\,\mathrm{Pr}$ on $\theta(\eta)$ is sketched in Fig. 7. Larger values of $N\,\mathrm{Pr}$ decrease the temperature profile and thermal boundary layer thickness. Modified Prandtl number involves the thermal diffusivity. Higher values of modified Prandtl number correspond to the weaker thermal diffusivity. Weaker thermal diffusivity shows lower temperature

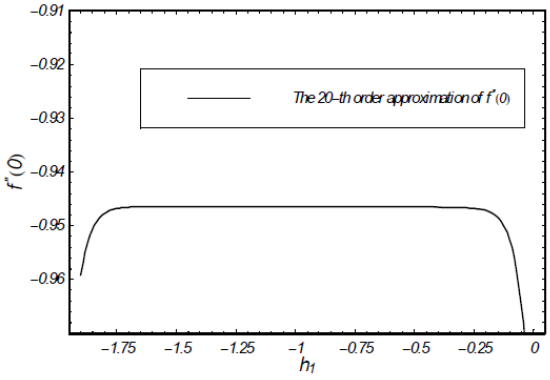

Fig. 1. $\hbar-curve$ for $f''(0)$.

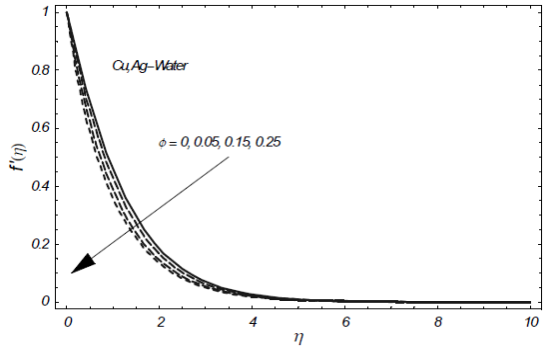

Fig. 3. Velocity profile for various values of φ when $k=1$ (Newtonian fluid) when $\lambda=1$.

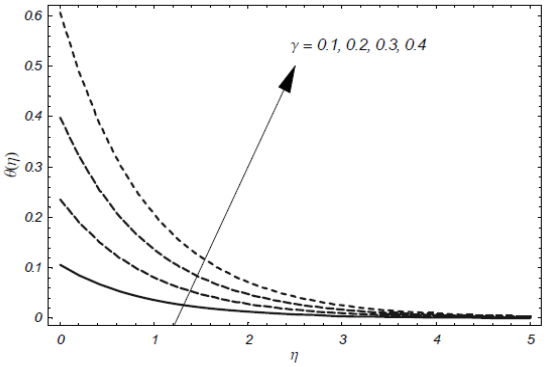

Fig. 5. Temperature profile for various values of γ when $k=1$ (Newtonian fluid), when $N\,\mathrm{Pr}=1;\lambda=1$ and $\phi=1$.

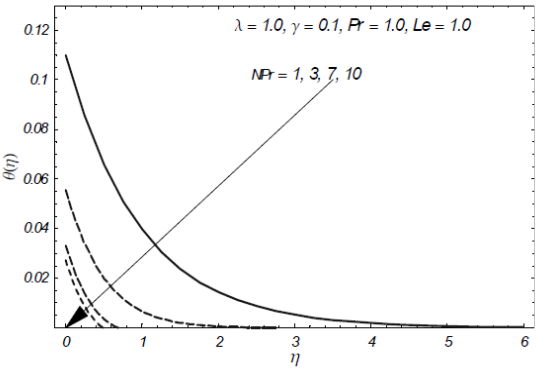

Fig. 7. Temperature profiles for various values of $N\,\mathrm{Pr}$ when $k=1$ (Newtonian fluid), when $\varphi=0.1;\lambda=1$ and $\gamma=0.1$.

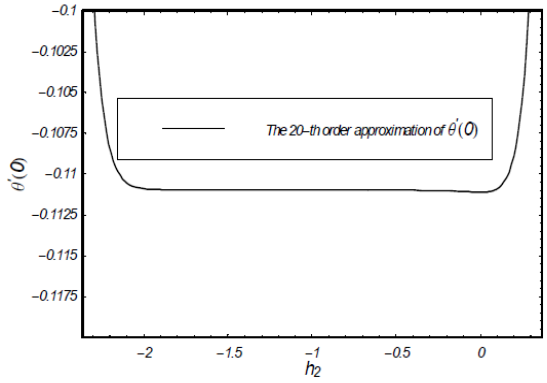

Fig. 2. $\hbar-curve$ for $\theta'(0)$.

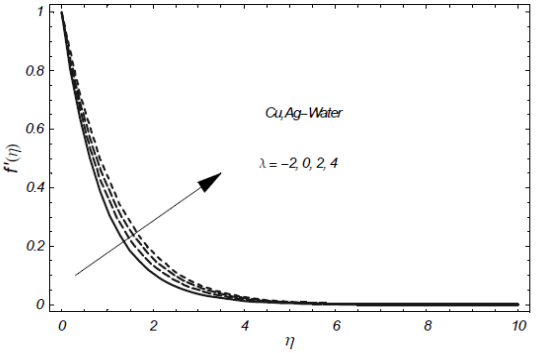

Fig. 4. Velocity profile for various values of λ when $k=1$ (Newtonian fluid) when $\varphi=1$

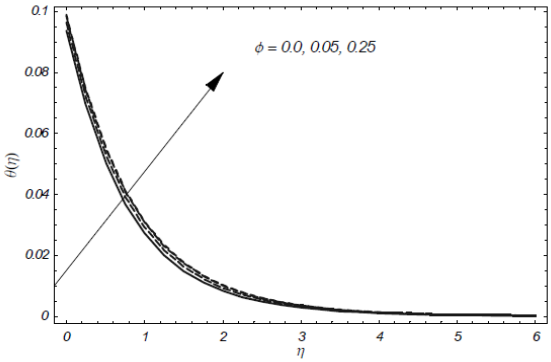

Fig. 6. Temperature profile for various values of φ when $k=1$ (Newtonian fluid), when $N\,\mathrm{Pr}=1;\lambda=1$ and $\gamma=1$.

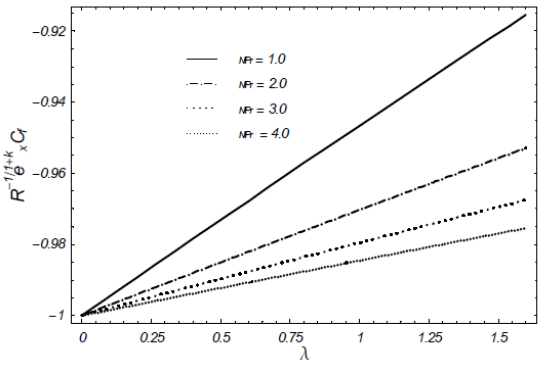

Fig. 8: Variation of skin friction for λ vs N Pr

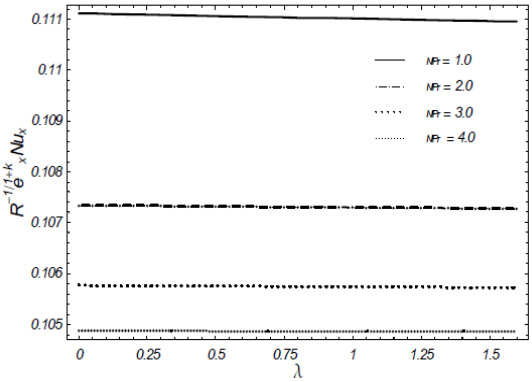

Fig. 9. Variation of Nusselt number for λ vs N Pr

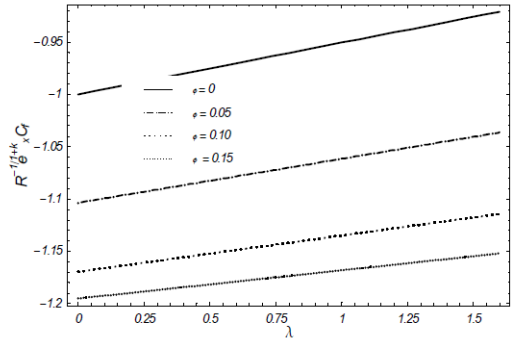

Fig. 10. Variation of skin friction for λ vs φ when N Pr = 1

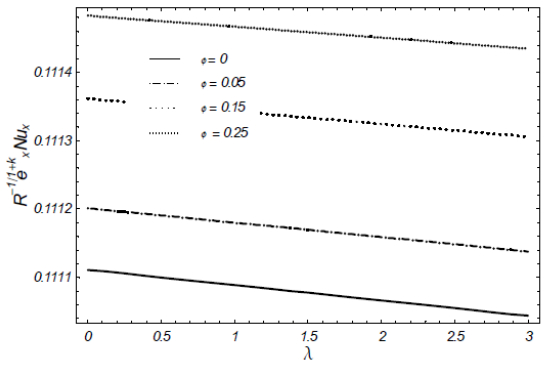

Fig. 11. Variation of Nusselt number for λ vs φ when N Pr = 1

Table 1 Convergence of the series solution at different order of approximations.

Order of approximations	$-f''(0)$	$-\theta'(0)$
1	0.50380	0.9855
10	0.52426	1.1841
15	0.52449	1.1841
20	0.52450	1.1841
25	0.52451	1.1842
30	0.52451	1.1842
40	0.52451	1.1842

Table 2 Numerical values of local Nusselt number $(\mathrm{Re}_x)^{-1/(k+1)} Nu_x$ of Cu-water nanofluid for different values of *NPr*, λ and γ.

NPr	λ	Γ	$(\mathrm{Re}_x)^{-1/(k+1)} Nu_x$	
			k=1.0	k=2.0
0.5	1.0	0.1	0.75197	0.76884
1.2			0.81142	0.82156
1.5			0.82234	0.83099
1.0	0.0	0.1	0.80000	0.81235
	2.0		0.80224	0.81301
	3.0		0.80328	0.81395
1.0	1.0	0.2	0.60513	0.62637
		0.3	0.41200	0.44091
		0.4	0.22209	0.25630

and thinner thermal boundary layer thickness. Variation of N Pr on skin friction and Nusselt number are shown in the Figs. 8 and 9. The skin friction increases through an increase in N Pr while Nusselt number decreases. Impact of volume fraction φ on skin friction and Nusselt number are shown in the Figs. 10 and 11. These Figs indicate that an increase in φ enhances the skin friction and Nusselt number.

4. CONCLUSIONS

We analyzed the boundary layer flow of power law nanofluid with Newtonian heating. The main points of this investigation are given below:

- Convergent solutions are obtained faster through Pade approximation.
- Increase in φ decreases the momentum boundary layer thickness but it increases for λ.
- Newtonian heating parameter γ and volume fraction φ increases the thermal boundary layer thickness.
- Momentum boundary layer thickness decreases for N Pr.
- The skin friction coefficient increases but Nusselt number decreases when the values of N Pr are increased.

- Volume fraction φ increases the skin friction coefficient and Nusselt number.

REFERENCES

Abbasbandy, S., Hashemi, M.S. and Hashim, I (2013). On convergence of homotopy analysis method and its application to fractional integro-differential equations, *Quaestiones Mathematicae*, 36, 93-105.

Chamkha, A.J. and Abu-Nada, E (2012). Mixed convection flow in single- and double-lid driven square cavities filled with water-Al_2O_3 nanofluid: Effect of viscosity models, *Europ. J. Mech. B/Fluids*, 36, 82-96.

Choi, S. U. S (1995). Enhancing thermal conductivity of fluids with nanoparticles, in: The Proceedings of the 1995 ASME. *Int. Mech. Eng. Congress and Exposition, SanFrancisco, USA, ASME, FED231/MD*, 66, 99-105

Hady, F.M., Ibrahim, F.S., Abdel-Gaied, S.M. and Eid, M.R (2011). Effect of heat generation/absorption on natural convective boundary-layer flow from a vertical cone embedded in a porous medium filled with a non-Newtonian nanofluid, *Int. Commun. Heat Mass Transfer*, 38, 1414-1420.

Hady, F.M., Ibrahim, F.S., Gaied, S.M.A. and Eid, M.R (2012). Radiation effect on viscous flow of a nanofluid and heat transfer over a nonlinearly stretching sheet, *Nanoscale Research Lett.*, 7, 229.

Hamad, M.A.A (2011). Analytical solution of natural convection flow of a nanofluid over a linearly stretching sheet in the presence of magnetic field, *Int. Commun. Heat Mass Transfer*, 38, 487-492.

Hayat, T., Iqbal, Z. and Mustafa, M (2012). Flow of a second grade fluid over a stretching surface with Newtonian heating, *J. Mech.*, 28, 209-216.

Hayat, T., Shehzad, S.A. and Alsaedi, A (2012). Soret and Dufour effects in magnetohydrodynamic (MHD) flow of Casson fluid, *Appl. Math. Mech.*, 33, 1301-1312.

Hayat, T., Shehzad, S.A., Al-Sulami, H.H. and Asghar, S (2013). Influence of thermal stratification on the radiative flow of Maxwell fluid, *J. Braz. Society Mech. Sci. Eng.*, 35, 381-389.

Hayat, T., Waqas, M., Shehzad, S.A. and Alsaedi, A (2013). Mixed convection radiative flow of Maxwell fluid near a stagnation point with convective condition, *J. Mech.*, 29, 403-409.

Ibrahim, W. and Makinde, O.D (2013). The effect of double stratification on boundary-layer flow and heat transfer of nanofluid over a vertical plate, *Comput. Fluids*, 86, 433-441.

Keimanesh, M., Rashidi, M.M., Chamkha, A.J. and Jafari, R (2011). Study of a third grade non-Newtonian fluid flow between two parallel plates using the multi-step differential transform method, *Comput. Math. Appl.*, 62, 2871-2891.

Liao, S.J (2003). Beyond perturbation: Introduction to the homotopy analysis method, *Chapman & Hall/CRC Press, Boca Raton*.

Makinde, O.D (2012). Computational modelling of MHD unsteady flow and heat transfer toward a flat plate with Navier slip and Newtonian heating, *Braz. J. Chem. Eng.*, 29, 159-166.

Makinde, O.D. and Aziz, A (2011). Boundary layer flow of a nanofluid past a stretching sheet with a convective boundary condition, *Int. J. Thermal Sci.*, 50, 1326-1332.

Mustafa, M., Hayat, T., Pop, I., Asghar, S. and Obaidat, S (2011). Stagnation point flow of nanofluid towards a stretching sheet. *Int. J. Heat Mass Transfer*, 54, 5588-5594.

Oztop, H.F., Abu-Nada, E., Varol, Y. and Al-Salem, K (2011). Computational analysis of non-isothermal temperature distribution on natural convection in nanofluid filled enclosures, *Superlattices Microstructures*, 49, 453-467.

Ramzan, M., Farooq, M., Alsaedi, A. and Hayat, T (2013). MHD three-dimensional flow of couple stress fluid with Newtonian heating, *Europ. Phys. J. Plus*, 128, 49.

Rashidi, M.M. and Domairry, G (2009). New analytical solution of the three dimensional Navier-Stokes equations, *Mod. Phys. Lett., B*, 23, 3147.

Rashidi, M.M., Abelman, S. and Mehr, N.F (2013). Entropy generation in steady MHD flow due to a rotating disk in nanofluid, *Int. J. Heat Mass Transfer*, 62, 515-525.

Rashidi, M.M., Hayat, T., Erfani, E., Pour, S.A.M. and Hendi, A.A (2011). Simultaneous effects of partial slip and thermal-diffusion and diffusion-thermo on steady MHD convective flow due to a rotating disk, *Commun. Nonlinear Sci. Numer. Simulat.*, 16, 4303-4317.

Rashidi, M.M., Rajvanshi, S.C. and Keimanesh, M (2012). Study of Pulsatile flow in a porous annulus with the homotopy analysis method, *Int. J. Num. Methods Heat Fluid Flow*, 22, 971-989.

Rashidi, M.M., Rastegari, M.T., Asadi, M., and Bég, O.A (2012). A study of non-Newtonian flow and heat transfer over a non-isothermal wedge using the homotopy analysis method, *Chem. Eng. Commun.*, 199, 231-256.

Salleh, M.Z., Nazar, R. and Pop, I (2010). Boundary layer flow and heat transfer over a stretching sheet with Newtonian heating, *J. Taiwan Institute Chem. Eng.*, 41, 651-655.

Shehzad, S.A., Hayat, T., Alhuthali, M.S. and Asghar S (2014). MHD three dimensional flow of Jeffrey

fluid with Newtonian heating, *J. Cent. South Univ.*, 21, 1428-1433.

Sheikholeslami, M., Gorji-Bandpy, M., Ganji, D.D. and Soleimani, S (2013). Natural convection heat transfer in a cavity with sinusoidal wall filled with CuO-water nanofluid in presence of magnetic field, *J. Taiwan Institute Chem. Eng.*, (in press).

Sheikholeslami, M., Hatami, M. and Ganji, D.D (2013). Analytical investigation of MHD nanofluidflow in a semi-porous channel, *Powder Technology*, 246, 327-336.

Turkyilmazoglu, M (2012). Exact analytical solutions for heat and mass transfer of MHD slip flow in nanofluids, *Chem. Eng. Science*, 84, 182-187.

Turkyilmazoglu, M (2012). Solution of the Thomas-Fermi equation with a convergent approach, *Commun. Nonlinear Sci. Numer. Simulat.*, 17, 4097-4103.

Turkyilmazoglu, M. and Pop, I (2013). Heat and mass transfer of unsteady natural convection flow of some nanofluids past a vertical infinite flat plate with radiation effect, *Int. J. Heat Mass Transfer*, 59, 167-171.